INTERNATIONAL JOURNAL FOR NUMERICAL METHODS IN FLUIDS, VOL. 17, 803–823 (1993)

SEMI-IMPLICIT SKEW UPWIND METHOD FOR PROBLEMS IN ENVIRONMENTAL HYDRAULICS

SIPING ZHOU, J. A. McCORQUODALE AND ZHONG JI

Department of Civil and Environmental Engineering, University of Windsor, 401 Sunset, Windsor, Ontario, Canada N9B 3P4

SUMMARY

A new computational method is presented for reducing numerical diffusion in environmental fluid problems. This method, which is referred to as the Semi-Implicit Skew Upwind Method (SISUM), is a robust solution procedure for the conditional convergence of the discretized transport equations. The method retains the advantage of the low numerical diffusion of the conventional skew upwind schemes but does not suffer from over- or under-shooting often found in these methods due to the improved interpolation schemes. The effectiveness of SISUM is demonstrated in several examples. The comparison of the results of a hybrid scheme and SISUM with field observations of convection-dominated pollutant transport in strongly curvilinear river flow shows that SISUM successfully eliminates the high numerical diffusion produced by the hybrid scheme. The robustness of the method was tested by solving the hydrodynamics of a circular clarifier model with a large density gravity source term in the vertical-momentum equation.

KEY WORDS Numerical diffusion Skew upwind Convective transport Stability

INTRODUCTION

The numerical solution of convection-dominated transport equations is plagued with several problems including instability, unrealistic oscillations and numerical diffusions. Success in overcoming the instability problem was first achieved through the use of upwind and hybrid schemes.[1] These schemes are still popular because of their robust nature but, the hybrid scheme suffers from severe numerical diffusion when the flow direction is not parallel to the local grid direction. For the case of a square grid, deVahl Davis and Mallinson[2] indicated that the numerical diffusion of a first-order upwind scheme is maximum when $\alpha = 45°$ (α = angle between velocity vector and co-ordinate axes).

Since Raithby[3] introduced the Skew Upwind Scheme (SUDS) to reduce the numerical diffusion, several SUDSs have been presented.[4–11] Although the SUDSs have been shown to minimize numerical diffusion, they have not been widely applied to solve environmental hydraulic problems such as elliptic river models. One reason for this is the complexity of the SUDSs compared to the hybrid scheme. However, the major difficulties in using conventional SUDSs in cases of low-level real diffusion are, the lack of a robust (stable) solution procedure and the occurrence of an anomaly in the form of over- or under-shooting. The value of the diagonal coefficient in skew methods is not always greater than (or equal to) the summation of the absolute values of the off-diagonal coefficients, due to the presence of the negative off-diagonal coefficients; consequently an unconditional convergency does not exist for the iterative solution of matrix equations. An absolutely stable iterative solution for a set of equations cannot be assured for all initial

0271–2091/93/210803–21$15.50

Received 16 June 1992
Revised 29 March 1993

assumptions, unless there is diagonal dominance.[12] Unfortunately, in some cases it is the smaller diagonal coefficients compared to the hybrid or the positive coefficient SUDSs that enable the conventional SUDSs to estimate more precisely the values of the convection flux on the Control-Volume (CV) faces.

In recent studies, the instabilities and over- or under-shooting problems have been improved by the following methods:

(1) The flux blending technique was proposed by Sturgess and Syed[8] and Peric *et al.*[10] This method calculates the convective flux as a weighted sum of the flux expressions from the first-order upwind and SUDSs. By lowering the weighting factor, the convected flux is calculated with more weight on the pure upwind scheme and therefore results in a positive increase in the coefficients and greater computational stability, but at the cost of more numerical diffusion.[13]
(2) The mass flow-weighted SUDS was first presented by Hassan *et al.*[4] and then Schneider and Raw.[7] This scheme guarantees positive equation coefficients but retains some, although significantly reduced, numerical diffusion.[9]
(3) The Non-linear Filtering Algorithm (FRAM) was presented by Sheu *et al.*[11] In this method, the high-order discretization of convection terms is the same as the conventional SUDS which allows negative coefficients to exist. The damping of numerical oscillations by the FRAM is achieved by selectively adding a strong local dissipation flux (numerical diffusion) to equations at the nodes where strong numerical oscillations appear. Sheu *et al.*[11] found that as the FRAM procedure is turned on, all the oscillations disappear but a dissipative error is added.

An alternative approach to achieving high-accuracy solutions is the QUICK method of Leonard.[14] The major differences between the QUICK and skew schemes are: (1) The QUICK principle distinguishes upstream nodes from downstream nodes based on the direction of the velocity component (u or v) at the face of CV, while the skew upwinding principle defines the upstream nodes along the direction of a streamline through a face of the CV; (2) the QUICK schemes use high-order accuracy interpolations in the defined upwind directions to obtain the face values (e.g. SMART,[15] ULTRA-QUICK/5th/7th[16]), while the skew methods have used linear interpolation. The application of the recent QUICK family with high-order accurate convection approximations [15,16] has successfully eliminated over- or under-shooting.

In this paper, a Semi-Implicit Skew Upwind Method (SISUM) is developed which yields positive coefficients in the coefficient matrix along with computational robustness without introducing extra-numerical diffusion or excessively large source terms involving the convection flux. Comparing the SISUM with all the skew upwinding methods cited in this paper, the major novel features of this method are:

(1) an extra iterative process which is designed to eliminate the numerical diffusion step by step while preventing the amplification of any deviations between the initial field and the final solution for the cases of non-dominant diagonal coefficients;
(2) improved convection flux expressions for the face values of the CV that do not yield over- or under-shooting.

INTEGRATING EQUATIONS OF THE SEMI-IMPLICIT SKEW UPWIND METHOD (SISUM)

The general two-dimensional water depth-averaged form of the convective-diffusion equation of a quantity φ in a body of water is

$$\frac{\partial \varphi}{\partial t}+u\frac{\partial \varphi}{\partial x}+v\frac{\partial \varphi}{\partial y}=\frac{1}{h}\frac{\partial}{\partial x}\left(h\frac{v_t}{\sigma_\varphi}\frac{\partial \varphi}{\partial x}\right)+\frac{1}{h}\frac{\partial}{\partial y}\left(h\frac{v_t}{\sigma_\varphi}\frac{\partial \varphi}{\partial y}\right)+S_\varphi, \tag{1}$$

in which u is the velocity component in the x-direction, v is the velocity component in the y-direction, v_t is the eddy viscosity, S_φ is the source term, h is the local water depth and σ_φ is the Schmidt number.

The dependent variables are discretized on the non-uniform staggered mesh as shown in Figure 1.[3] The integration of equation (1) over the CV (Figure 1) yields[17]

$$\int_{\mathrm{Vol}}\frac{\partial \varphi}{\partial t}\mathrm{dVol}+[\varphi_e(uh)_e\mathrm{d}y_P-\varphi_w(uh)_w\mathrm{d}y_P]+[\varphi_n(vh)_n\mathrm{d}x_P-\varphi_s(vh)_s\mathrm{d}x_P]$$

$$=\int_{\mathrm{Vol}}(\text{diffus. terms})\,\mathrm{dVol}+\int_{\mathrm{Vol}}S_\varphi\mathrm{dVol}, \tag{2}$$

where u_e and u_w are the velocity components in the x-direction at the control-volume surface points e and w, respectively, and v_n and v_s are the velocity components in the y-direction at the surface points n and s, respectively.

The SISUM chooses implicit expressions for the convection flux for the influent surfaces of the CV and semi-implicit expressions for the effluent surfaces. The term semi-implicit refers to the fact that the effluent fluxes involve the old values of φ_P. In SISUM, the effluent convection flux terms are placed on the left-hand side of the equation to distinguish them from the influent terms which appear on the right-hand side. Four possible skew flows are considered, i.e. NE, NW, SE and SW (Figure 1).

In the SW case ($u_e\geq 0$, $u_w\geq 0$, $v_n\geq 0$ and $v_s\geq 0$), the CV faces w and s are the convection flux inlet faces while faces e and n are the outlet faces. The conservation equation including the convected flux through the CV is obtained from equation (2) as

$$\varphi_eF_e+\varphi_nF_n=\varphi_wF_w+\varphi_sF_s+\int_{\mathrm{Vol}}(\text{diffus. terms}+S_\varphi-\partial\varphi/\partial t)\mathrm{dVol}. \tag{3}$$

Similarly, for the SE case ($u_e\leq 0$, $u_w\leq 0$, $v_n\geq 0$ and $v_s\geq 0$), equation (2) becomes

$$\varphi_wF_w+\varphi_nF_n=\varphi_eF_e+\varphi_sF_s+\int_{\mathrm{Vol}}(\text{diffus. terms}+S_\varphi-\partial\varphi/\mathrm{d}t)\mathrm{dVol}. \tag{4}$$

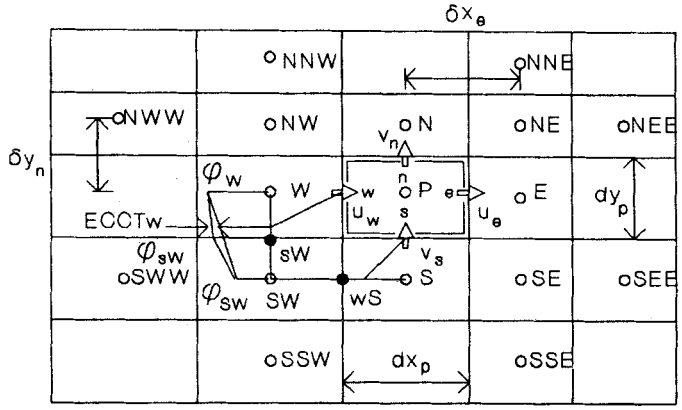

Figure 1. Control volume with 17 surrounding nodal points

For the NW and NE cases ($u_e \geq 0$, $u_w \geq 0$, $v_n \leq 0$ and $v_s \leq 0$, and $u_e \leq 0$, $u_w \leq 0$, $v_n \leq 0$ and $v_s \leq 0$, respectively), one obtains

$$\varphi_e F_e + \varphi_s F_s = \varphi_w F_w + \varphi_n F_n + \int_{\text{Vol}} (\text{diffus. terms} + S_\varphi - \partial\varphi/\mathrm{d}t)\,\mathrm{dVol} \tag{5}$$

and

$$\varphi_w F_w + \varphi_n F_n = \varphi_e F_e + \varphi_s F_s + \int_{\text{Vol}} (\text{diffus. terms} + S_\varphi - \partial\varphi/\mathrm{d}t)\,\mathrm{dVol}, \tag{6}$$

where the flows of the convection flux F_n, F_s, F_e and F_w on the four CV faces are

$$F_e = |u_e| h_e \,\mathrm{d}y_P; \qquad F_w = |u_w| h_w \,\mathrm{d}y_P \tag{7}$$

and

$$F_n = |v_n| h_n \,\mathrm{d}x_P; \qquad F_s = |v_s| h_s \,\mathrm{d}x_P. \tag{8}$$

A few cell-flow anomalies, such as cell trifurcation flow with three inlet or outlet faces, cell stagnation flow and cell counter-flow, may occur in the computation domain. For these rare cases, the cell flow regime loses its strong and unique directional feature. An average velocity vector direction at the centre of the cell was used in SISUM instead of the individual vector directions at the faces to overcome this local anomaly. In the small sub-domain associated with these cell anomalies, this approximation can still give reasonable accuracy since diffusion processes are usually dominant over convection.

The following derivation focuses on the SW case including the diffusion as well as transient and source terms. Similar discretization procedures can easily be extended for the other three cases.

Using second-order central differencing to discretize the diffusion terms in equation (3) gives

$$\varphi_e F_e + \varphi_n F_n + D_p \varphi_P = \varphi_w F_w + \varphi_s F_s + D_e \varphi_E + D_w \varphi_W + D_s \varphi_S + D_n \varphi_N + (S_\varphi + \varphi_P^0/\Delta t) h_P \mathrm{d}x_p \mathrm{d}y_p \tag{9}$$

where the lower case subscripts are for the face values, the upper case subscripts are for the values at grid nodes, and φ_P^0 is the value of φ_P from the previous time step. The diffusion fluxes D_n, D_s, D_e and D_w on the four CV faces and the coefficient D_p are given as

$$D_e = \left(\frac{\nu_t}{\sigma_\varphi}\right)_e h_e \mathrm{d}y_p/\delta x_e; \qquad D_w = \left(\frac{\nu_t}{\sigma_\varphi}\right)_w h_w \mathrm{d}y_p/\delta x_w, \tag{10}$$

$$D_s = \left(\frac{\nu_t}{\sigma_\varphi}\right)_s h_s \mathrm{d}x_p/\delta y_s; \qquad D_n = \left(\frac{\nu_t}{\sigma_\varphi}\right)_n h_n \mathrm{d}y_p/\delta y_n, \tag{11}$$

$$D_p = D_e + D_w + D_s + D_n + \mathrm{d}x_p \mathrm{d}y_p h_P/\Delta t. \tag{12}$$

The closure-conservation equation (9) requires estimates of the convection fluxes of φ across the CV faces; this means that the values φ_e, φ_n, φ_w and φ_s are determined from the surrounding nodal values such as φ_P, φ_W, φ_{SW} and φ_S, as shown in Figure 2. The upwinding along the streamline direction is chosen to relate the nodal variables to the CV face points.

CONVECTION EXPRESSIONS OF CONVENTIONAL SUDS

For a steady pure convection problem, equation (1) can be re-written in the local streamwise direction, s, as

$$\rho V_s (\partial\varphi/\partial s) = 0 \tag{13}$$

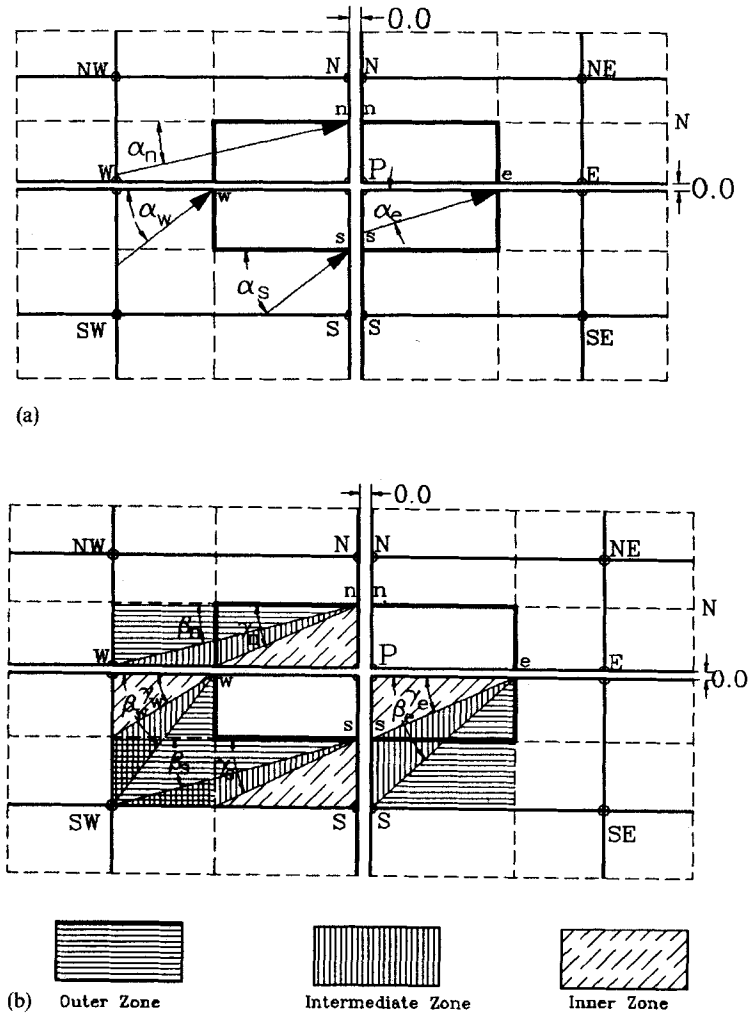

Figure 2. Illustration of interpolation method of SISUM: (a) velocity angles at four faces of the control volume; (b) critical angles of SISUM

where

$$V_s=(u^2+v^2)^{1/2}; \qquad \mathrm{d}s=\left(\frac{u}{V_s}\mathrm{d}x,\frac{v}{V_s}\mathrm{d}y\right). \tag{14}$$

Considering the inlet surface point w as an example, the general form of equation (13) can be given as [9]

$$\rho V\frac{\partial\varphi}{\partial s}\doteq\rho V\frac{(\varphi_w-\varphi_u)}{L}\doteq 0; \quad \varphi_w\doteq\varphi_u, \tag{15}$$

for the flow direction shown in Figure 2(a). The subscript u on φ means 'upwind' and L is the path length.

For the SW case the estimates of the convection flux used in the conventional SUDS[3,11] at faces s and w give

$$\varphi_s = A_s^1 \varphi_{SW} + (1{\cdot}0 - A_s^1)\varphi_W (\alpha_s < \beta_s); \qquad \varphi_s = A_s \varphi_{SW} + (1{\cdot}0 - A_s)\varphi_S (\alpha_s \geq \beta_s), \tag{16}$$

$$\varphi_w = A_w \varphi_{SW} + (1{\cdot}0 - A_w)\varphi_W (\alpha_w \leq \beta_w); \qquad \varphi_w = A_w^1 \varphi_{SW} + (1{\cdot}0 - A_w^1)\varphi_S (\alpha_w > \beta_w), \tag{17}$$

where A_w (along the line W–SW), A_s (along the line S–SW), A_w^1 (along the line S–SW) and A_s^1 (along the line W–SW) are linear interpolation factors, α_w is the angle between the velocity vector at point w and line w–P, α_s is the angle between the velocity vector at point s and the CV face s as shown in Figure 2(a), and β_w and β_s are shown in Figure 2(b). The remaining faces are treated in a similar manner. This scheme can result in up to 30% over- or under-shooting even when the negative coefficients are reduced by cutting off the skew scheme at the corner point in Raithby's original procedure (see Appendix I).

CONVECTION EXPRESSIONS OF SISUM

Outlet faces

Figure 2(b) shows the three possible zones where the velocity vector can fall. These are defined as the inner zone, the intermediate zone and the outer zone. In order to eliminate under- or over-shooting, the strategy of SISUM for the two outlet expressions is to use: (a) single node skew upwinding for outer zone (cutting off the scheme at the corner point), (b) two node skew upwinding for intermediate angles and (c) mixed nodal and face point skew upwinding for the inner zone. The angles α, β and γ shown in Figures 2(a) and 2(b) are all measured in the counter-clockwise direction from the horizontal grid.

The SISUM estimates of the convected flux through the two outlet faces are

$$\begin{aligned} &\varphi_n = A_n^{11}\varphi_w + (1{\cdot}0 - A_n^{11})\varphi_P \qquad (\alpha_n \geq \gamma_n), \\ &\varphi_n = A_n \varphi_W + (1{\cdot}0 - A_n)\varphi_P \qquad (\beta_n \leq \alpha_n < \gamma_n), \\ &\varphi_n = \varphi_W \qquad (\alpha_n < \beta_n) \end{aligned} \tag{18}$$

and

$$\begin{aligned} &\varphi_e = A_e^{11}\varphi_s + (1{\cdot}0 - A_e^{11})\varphi_P \qquad (\alpha_e \leq \gamma_e), \\ &\varphi_e = A_e \varphi_S + (1{\cdot}0 - A_e)\varphi_P \qquad (\beta_e \geq \alpha_e > \gamma_e), \\ &\varphi_e = \varphi_S \qquad (\alpha_e > \beta_e), \end{aligned} \tag{19}$$

where α_e is the angle between the velocity vector at point e and line e–P, α_n is the angle between the velocity vector at point n and the control-volume face n (Figure 2(a)), β_e, β_n, γ_e and γ_n are the critical angles as shown in Figure 2(b), and A_e (along the line P–S), A_e^{11} (along the line P–s), A_n and A_n^{11} are linear interpolation factors.

Inlet faces for nine-point SISUM

For the two inlet expressions, (a) single node skew upwinding is used for the outer zone and (b) two node skew upwinding is used for the intermediate and inner zones (Figure 2(b)). The estimates of the convection flux through the two inlet faces are given by

$$\varphi_w = A_w \varphi_{SW} + (1{\cdot}0 - A_w)\varphi_W \quad (\alpha_w \leq \beta_w); \qquad \varphi_w = \varphi_{SW} \quad (\alpha_w > \beta_w) \tag{20}$$

and

$$\varphi_s = A_s \varphi_{SW} + (1{\cdot}0 - A_s)\varphi_S \quad (\alpha_s \geq \beta_s) \qquad \varphi_s = \varphi_{SW} \quad (\alpha_s < \beta_s), \tag{21}$$

where α_w is the angle between the velocity vector at point w and the line w–W; α_s is the angle between the velocity vector at point s and the control-volume face s, β_w and β_s are the critical angles as shown in Figure 2(b), and A_w and A_s are linear interpolation factors.

This version of SISUM is a partially conservative scheme (SISUM-9) and although it is simple to apply and effective in reducing over- and under-shooting, it has the disadvantage of being partially non-conservative when the velocity vector is in the inner zone (e.g. $\alpha_e < \gamma_e$). This can be seen from the expression for the flux leaving Control Volume P (CVP) through the face e, which is different from the expression for the flux entering CVE through the same face. However, if the same expression was used for inlet faces as was used for the outlet faces, the final discretization equations could directly involve 17 grid nodes. For an implicit or semi-implicit skew upwind scheme, the computer code would be extremely difficult since all the face expressions, being dependent on the variable local velocity directions, would yield a huge number of possible combinations of different nodes.

Inlet faces for seventeen-point SISUM

The non-conservative error in SISUM-9 is produced by the difference between two values on the same face given by expressions with different interpolation accuracies (e.g. when $\alpha_e < \gamma_e$); consequently, this error can be significantly reduced by reduction of the grid size, and it will be less important in problems with low gradients. To overcome this partially non-conservative problem without unduly complicating the code, two semi-implicit expressions for the inlet faces w and s are introduced:

$$\begin{aligned}
&\varphi_w = A_w \varphi_{SW} + (1{\cdot}0 - A_w)\varphi_W + \mathrm{ECCT}_w \qquad (\alpha_w \leq \gamma_w),\\
&\varphi_w = A_w \varphi_{SW} + (1{\cdot}0 - A_w)\varphi_W \qquad (\gamma_w < \alpha_w \leq \beta_w),\\
&\varphi_w = \varphi_{SW} \qquad (\alpha_w > \beta_w)
\end{aligned} \tag{22}$$

and

$$\begin{aligned}
&\varphi_s = A_s \varphi_{SW} + (1{\cdot}0 - A_s)\varphi_S + \mathrm{ECCT}_s \qquad (\alpha_s \geq \gamma_s),\\
&\varphi_s = A_s \varphi_{SW} + (1{\cdot}0 - A_s)\varphi_S \qquad (\beta_s \leq \alpha_s < \gamma_s),\\
&\varphi_s = \varphi_{SW} \qquad (\alpha_s < \beta_s),
\end{aligned} \tag{23}$$

where ECCT_w is the 'Explicit Conservative Compensation Term at face w'

$$\mathrm{ECCT}_w = \varphi^{W}_{\mathrm{out}-w}(\varphi_{SW}, \varphi_W) - \varphi^{P}_{\mathrm{in}-w}(\varphi_{SW}, \varphi_W) \tag{24}$$

where $\varphi^{W}_{\mathrm{out}-w}$ is the face value leaving Control Volume W (CVW) through the face w, $\varphi^{P}_{\mathrm{in}-w}$ is the face value entering CVP through the same face, and φ_{SW} is the face value entering CVW through the face sW, as shown in Figure 1. Similarly, ECCT_s is the 'Explicit Conservative Compensation Term at face s', i.e.

$$\mathrm{ECCT}_s = \varphi^{S}_{\mathrm{out}-s}(\varphi_{WS}, \varphi_S) - \varphi^{P}_{\mathrm{in}-s}(\varphi_{SW}, \varphi_S), \tag{25}$$

where $\varphi^{S}_{\mathrm{out}-s}$ is the face value leaving CVS through the face s, $\varphi^{P}_{\mathrm{in}-s}$ is the face value entering CVP through the same face, and φ_{WS} is the face value entering control volume S through the face wS, as shown in Figure 1. The final four sets of convection-flux expressions will implicitly involve nine

centre nodes and explicitly involve another eight nodes around the nine centre nodes due to the four possible skew directions (see Figure 1). Equations (18), (19), (22) and (23) give a fully conservative SISUM (SISUM-17). The code of SISUM-17 computes any residuals between the inlet-face values of the current CV (given by equations (20) and (21)) and the outlet face values corresponding to the two upwind CVs. These residuals, which are much smaller than the convection term itself, are added to the source term of the final discretization equation of SISUM-17.

FINAL DISCRETIZATION EQUATION OF SISUM

The influent convection flux expressions (Equations (20) and (21) or (22) and (23)) can be introduced directly into the right-hand side of equation (9) to replace the surface values φ_w and φ_s without producing negative off-coefficients. However, when the effluent convection flux expressions (equations (18) and (19)) are directly used to replace the values φ_e and φ_n on the left-hand side of equation (9), then negative convection terms from the left-hand side of the equation (such as φ_S and φ_W) may give a final coefficient matrix with negative values (see Appendix I). The reduced diagonal coefficient resulting from the negative off-diagonal coefficients may lead to instability; this problem is different from the over- or under-shooting generated by the *convection* approximation.[16]

This problem is solved by using a unique property of node P which is evident when the two oulet faces of the CV are distinguished from the two inlet faces. Node P is always an upwind point to the two outlet faces regardless of the flow direction. The distance from node P to the outlet faces is the shortest in comparison to the distances from other upwind nodes. Based on this property, the effluent values of φ_e and φ_n are assumed to be proportional to the centre-nodal value φ_P given as

$$\varphi_e = C_e \varphi_P; \qquad \varphi_n = C_n \varphi_P, \tag{26}$$

where C_e and C_n are two unknown proportionality coefficients which depend on the distribution of φ on the respective effluent faces. Substitution of expressions (equation (26)) for the effluent convection terms in equation (9) leads to

$$(C_e F_e + C_n F_n + D_p)\varphi_P = F_w f(\varphi_W, \varphi_{SW}) + F_s f(\varphi_S, \varphi_{SW}) + F_w \mathrm{ECCT}_w + F_s \mathrm{ECCT}_s + D_e \varphi_E + D_w \varphi_W + D_s \varphi_S + D_n \varphi_N + (S_\varphi + \varphi_P^0/\Delta t) h_P \mathrm{d}x_p \mathrm{d}y_p, \tag{27}$$

where ECCT_w and ECCT_s are zero for SISUM-9. The terms of $F_w f(\varphi_W, \varphi_{SW})$ and $F_s f(\varphi_S, \varphi_{SW})$ represent four different combinations of the branches in equations (22) and (23) for the SW case; they are not source terms. In the computer code, equation (27) is replaced by four individual expressions corresponding to: (1) $\alpha_w \le \beta_w$, $\alpha_s \le \beta_s$; (2) $\alpha_w \le \beta_w$, $\alpha_s \ge \beta_s$; (3) $\alpha_w \ge \beta_w$, $\alpha_s \le \beta_s$; (4) $\alpha_w \ge \beta_w$; $\alpha_s \ge \beta_s$.

To estimate the effluent distribution coefficients C_e and C_n, we start with the assumption of uniform distribution of φ on the two effluent surfaces, i.e. $C_e = C_n = 1$, which means that the quantity φ is well mixed in the CV. The assumption that $\varphi_e = \varphi_n = \varphi_P$ for the effluent surfaces corresponds to the first-order upwind scheme. This initial approximation is referred to as a 'Mixed skew upwind scheme' which possesses the property of unconditional convergency; however, it still retains some numerical diffusion due to the assumption of uniform distribution on the two effluent surfaces. The accurate expressions of the 'non-uniform effluent distribution coefficients' are

$$C_e = \frac{\varphi_e}{\varphi_P^*}; \qquad C_n = \frac{\varphi_n}{\varphi_P^*}, \tag{28}$$

in which φ_e and φ_n through the two outlet faces are given by equations (18) and (19), and the superscript * on φ_P is for the old value at each iterative step. The final discretization equation for SISUM-9/17 is

$$\left(\frac{\varphi_e}{\varphi_P^*}F_e+\frac{\varphi_n}{\varphi_P^*}F_n+D_p\right)\varphi_P=F_w f(\varphi_W,\varphi_{SW})+F_s f(\varphi_S,\varphi_{SW})+F_w\mathrm{ECCT}_w+F_s\mathrm{ECCT}_s$$
$$+D_e\varphi_E+D_w\varphi_W+D_s\varphi_S+D_n\varphi_N+(S_\varphi+\varphi_P^0/\Delta t)h_P\,\mathrm{d}x_p\,\mathrm{d}y_p. \tag{29}$$

When the iterations converge, i.e. as φ_P approaches φ_P^*, equation (29) satisfies the original equation (9) and gives the solution with the lowest level of numerical diffusion. When the φ_p^* tends to zero, the analytical values of equation (28) will tend to be infinite; a zero solution for φ_p of equation (29) will be obtained by the iterative solution process which is absolutely robust due to the highly dominant diagonal coefficient. In practice, a very small value (10^{-30}) should be added to φ_P^* in the computer code to avoid dividing by zero.

The algorithm (equation (29)) has the property that an over-estimate of φ_p yields the stabilizing downward compensation from $C_e+C_n>2$ at each iteration, while an under-estimate of φ_p gives an upward compensation since $C_e+C_n<2$. In contrast with the conventional SUDS which starts by solving a conditionally convergent equation for an arbitrary given initial field, the SISUM allows some numerical diffusion to exist at the beginning of the iteration to obtain an unconditionally convergent equation. The remaining numerical diffusion is gradually minimized as the estimated non-uniform distribution coefficients C_e and C_n approach their true values, which may be less than one. This method delays the solution of the final conditionally stable equation (in which the summation of the local C_e and C_n may decrease to the minimum value) until the initial field is sufficiently close to the final solution to prevent divergence.

APPLICATIONS OF THE SEMI-IMPLICIT SKEW UPWIND METHOD (SISUM)

Pure convection of an oblique step

Comparative testing. Numerical diffusion can be studied by setting the real diffusion to zero in a transport problem that has an analytical solution. For a pure convection problem, an imposed concentration discontinuity should persist in the streamwise direction. The simulation of the pure convection of an oblique concentration discontinuity has been discussed by Patankar[17] and has been used as a test case by Raithby,[3] Ramadhyani and Patankar,[5] Raw,[6] Gaskell and Lau,[15] Leonard and Mokhtari[16] and Sheu *et al.*[11]

The results of the SISUM-9/17 are compared with those of Raw using the same square and uniform 11×11 grid. A uniform velocity is imposed at an angle α to the horizontal grid; the discontinuity step, $\varphi=1$ to $\varphi=0$, passes through the centre of the computational mesh, as shown in Figure 3(a). Figures 3(a)–3(c) show the results of the hybrid, mixed skew upwind and SISUM-17 for the case of $\alpha=45°$, which is the worst situation for the hybrid scheme. Figure 3(b) shows the initial field of SISUM-17 which was obtained by assuming $C_e=C_n=1{\cdot}0$ (mixed skew upwind). The iterative convergence rate, at the central point of the computation domain (exact solution $\varphi=1{\cdot}0$), is shown in Figure 4. The result indicates that after 20 iterative steps SISUM-17 practically eliminates the imposed numerical diffusion in the initial field. The final result accurately reproduces the discontinuous φ profile and is the same as that of the conventional skew upwind scheme.[6] SISUM-9 gives the same result as SISUM-17 since both schemes are the same for $\alpha=45°$. By contrast, the results predicted by positive coefficient skew upwind methods and conventional SUDS with FRAM[11] (Grid 50×50) show that some numerical diffusion

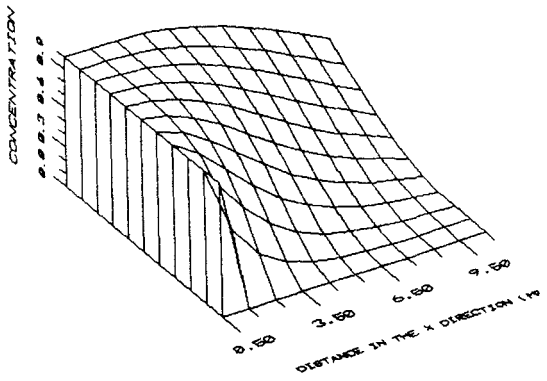

(a) Prediction by Hybrid scheme

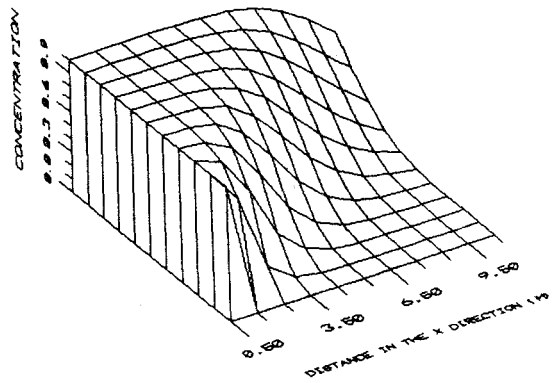

(b) Prediction by Mixed Skew Upwind scheme

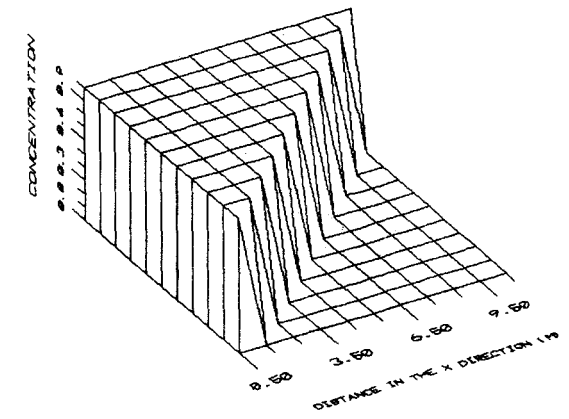

(c) Prediction by SISUM-9/17

Figure 3. Transport of an oblique concentration discontinuity in a uniform velocity region for $\alpha = 45°$ ($Y_c = 0{\cdot}0$) and grid 11×11: (a) prediction by hybrid scheme; (b) prediction by mixed skew upwind scheme; and (c) prediction by SISUM-9/17

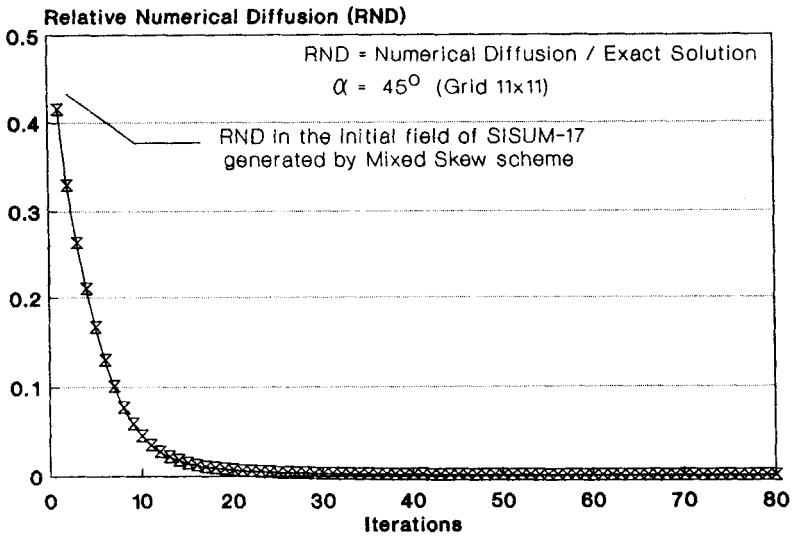

Figure 4. Iterative convergence of SISUM-17 at the central point of the calculation domain

remained for this case. Also, the results of SISUM-9/17 are better than those given by standard QUICK and SMART[15] (grid 21×21) when $\alpha = 45°$.

Figures 5(a)–5(c) show the results of the hybrid, SISUM-9 and SISUM-17, respectively, for the case of $\alpha = 31°$. For this case, the convection approximation of SISUM-17 is different from the SISUM-9 due to $\alpha_c < \gamma_c$ (inner zone). SISUM-17 shows almost no numerical diffusion in the result while SISUM-9 shows some numerical diffusion due to the partially non-conservative nature of this scheme and the very coarse grid. Both SISUM schemes give much better results than the hybrid. Furthermore, neither SISUM-9 nor SISUM-17 generated any under- or over-shooting.

In order to compare the results of SISUM-9/17 with Raw's results, the case of $\gamma_c = 8{\cdot}0$ ($\alpha = -31°$) was considered where the boundary value of φ between boundary conditions $\varphi = 1$ and $\varphi = 0$ was set to 0·5.[3,5,6] Figure 6 compares the profiles predicted by the regular SUDS,[6] the positive coefficient skew upwind (the mass flow-weighted skew upwind scheme),[6] SISUM-9 and SISUM-17 with the exact solution at a central vertical plane. The solutions of SISUM-9 display lower smearing than the positive coefficient skew upwind method. At grid points 0, 1, 2, 3 and 7, 8, 9, 10, SISUM-9 gives solutions that are better or the same as the conventional SUDS, but the conventional SUDS suffers from an over- and under-shoot of about 5%–10% for an 11×11 grid[6] and about 15%–25% for a 50×50 grid.[11] At grid points 4 and 6, the solutions of conventional SUDS seem to have lower numerical diffusion than SISUM-9; however, the conventional results at these two points may not be the true solutions of the original discretization equation due to unrealistic compensations from the over- or under-shooting at points 3 and 7. Again, SISUM-17 shows a promising result even for this very coarse grid.

Computational efficiency. Because of the significant additional operation-count per grid-point, the cost of SISUM-9/17 per grid-point for each iteration is 1·4–1·6 times that of the hybrid scheme. However, on comparing the result given by SISUM (number of nodes, $N = 11 \times 11$) with that given by hybrid scheme ($N = 50 \times 50$) for the case presented in Figure 3(c) ($\alpha = 45°$), it was found that the result of SISUM is still much better than that of the hybrid scheme despite the N used in the hybrid scheme being 20 times that used by SISUM.[18] For each iteration, the

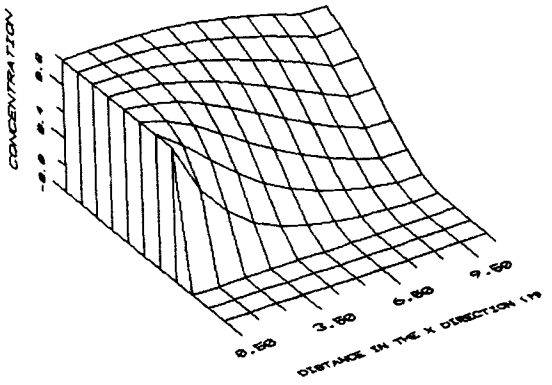

(a) Prediction by Hybrid scheme

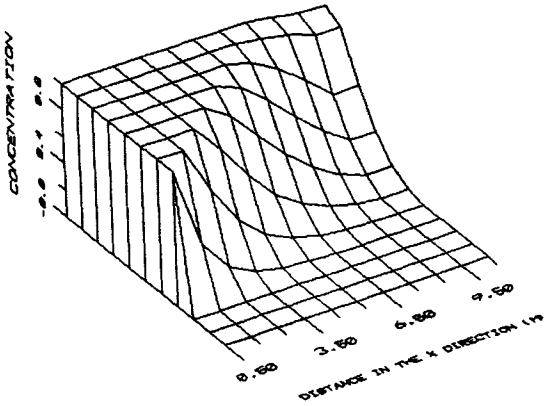

(b) Prediction by SISUM-9

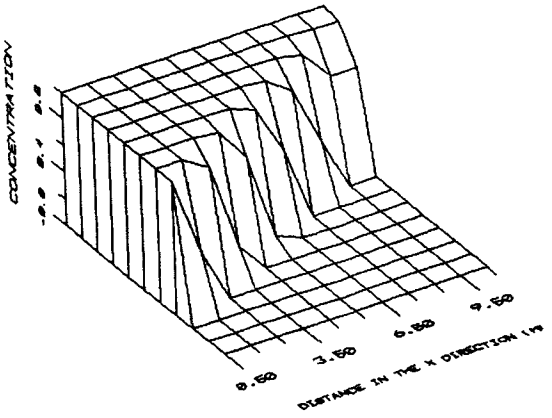

(c) Prediction by SISUM-17

Figure 5. Transport of an oblique concentration discontinuity in a uniform velocity region for $\alpha = 31°$ ($Y_c = 2{\cdot}0$) and grid 11×11: (a) prediction by hybrid scheme; (b) prediction by SISUM-9; and (c) prediction by SISUM-17

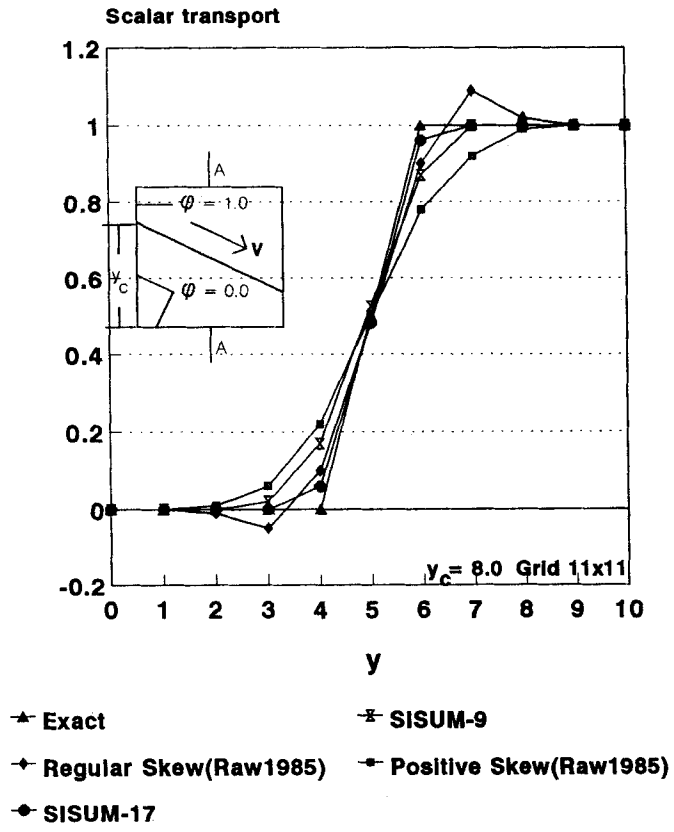

Figure 6. Transport of an oblique concentration discontinuity in a uniform velocity region for $\alpha = -31°$ ($Y_c = 8{\cdot}0$) and grid 11×11

relative CPU time required for $N = 50 \times 50$ is 20 (if TDMA is used) or 400 (Gaussian algorithm) times that required for $N = 11 \times 11$. Furthermore, for a practical problem with recirculations and diffusion, the iterative steps required to achieve convergence for either the hybrid scheme or SISUM are typically proportional to N^2. Since the explicit skew upwind method has a large convection source term, its time step must be very small. For a given level of numerical diffusion, the computational efficiency of SISUM is higher than either the explicit skew upwind method or the hybrid scheme. The fully implicit SUDS could result in a higher computational efficiency than SISUM, but instability problems may be encountered due to non-dominant diagonal coefficients.

Pollutant spreading in the Detroit River

SISUM-9/17 is applied to the simulation of pollutant transport in the Detroit River to illustrate its effectiveness in solving an environmental problem.

Governing equations. The two-dimensional depth-averaged unsteady model, adopted here, consists of two elliptic momentum equations along with the continuity equation for the primitive hydrodynamic variables and an elliptic conservation equation for the contaminant mass. The turbulent transport terms that appear in these equations are determined with the aid of the k–ε

model.[19] The standard parameters in the k–ε model can be used for large or small rivers with acceptable accuracy. The mixing length theory could have been used but this would require calibration for each river problem. The mathematical model is the same as that of Rodi[19] except that SISUM-9/17 replaces the hybrid scheme for solving the elliptic equations. The pressure can be solved as a general 2D problem by using the SIMPLE method[17] and the 'rigid-lid' assumption. The pressure difference is converted to the deviation of the surface elevation by the hydrostatic assumption. The pressure solution process is faster than directly solving an unsteady water depth-average continuity equation.

Calculation domain and boundary conditions. The hydraulics of the Detroit River was treated in two steps: (a) both Detroit and Fleming Channels were computed by a relatively coarse grid including Belle Isle and Peach Island (see Figure 7); (b) a refined grid is applied to simulate the Fleming Channel. The coarse grid yielded the upstream inlet boundary condition C–C (see Figure 8) for the Fleming Channel.

The reach of the Fleming Channel simulated in the second step extended from Lake St.Clair to 11 070 m downstream. The width of the calculation domain was 3307 m; a 67×47 non-uniform grid was used. The length for each CV in the lateral direction of the river was in the range 67·5–135 m while in the longitudinal direction the range was 90–270 m.

Based on the field data in the Detroit River,[20] the total discharge was 6230 $m^3 s^{-1}$, the inflow Q_1 to the Detroit Channel was 3993 $m^3 s^{-1}$, and the inflow Q_2 to the Fleming Channel was 2237 $m^3 s^{-1}$. The field velocity data at the inflow boundary were adjusted to obtain the inflow boundary condition.

The inflow concentration profile varied from 100 units at the Windsor river bank to 20 units at 405 m offshore.

SISUM-9 was used for boundary CVs while either SISUM-9 or SISUM-17 can be used for the internal CVs. Additional 'IF' statements are required in the code to consider the differences between the boundary CVs and internal CVs due to the staggered grid. The cases considered are: (1) one face of the boundary CV has a solid wall, and for this case the face point has the same position as the boundary node and critical angle β should be equal to γ when equations (18) to (21) are used; (2) the solid wall is treated as an inlet or outlet face with zero convection flux; (3) the hybrid scheme is used for the cases of two or three solid walls at boundary faces.

Hydrodynamics. Figure 8 shows the predicted flow pattern in the Fleming Channel for the refined grid using SISUM-9. Two major recirculation zones and a still water zone were predicted. The first recirculation zone at the point A1 is caused by the main stream separating from the bank due to local shoreline curvature. The second eddy occurs near the Belle Isle side (Point A2); the strength of the eddy is relatively weak due to the shallow local water depth (0·8–1·5 m). Figure 9 compares the velocity profiles predicted by SISUM-9 and hybrid with the field data of the U.S. Army Corps of Engineers[20] at section A2–A2′ (see Figure 8). Both the model and field data give main-stream velocities, which are fairly uniform, in the range 0·7–0·9 $m s^{-1}$. The strength and size of the recirculation zone and the associated lateral velocity gradients simulated by SISUM-9 are greater than those predicted by the hybrid scheme due to the lower numerical diffusion of SISUM-9.

Pollutant distribution. The aerial photograph shown in Figure 7 was taken by the Canadian Air Photo Service in 1976 just after a storm on Lake St. Clair. The turbidity plume was caused by the resuspension of fine sediment in the near-shore region along the transition from the lake to the Fleming Channel of the Detroit River. A significant feature of the turbidity plume is its slow rate of transverse mixing.

Figure 7. Turbidity plume in Fleming Channel

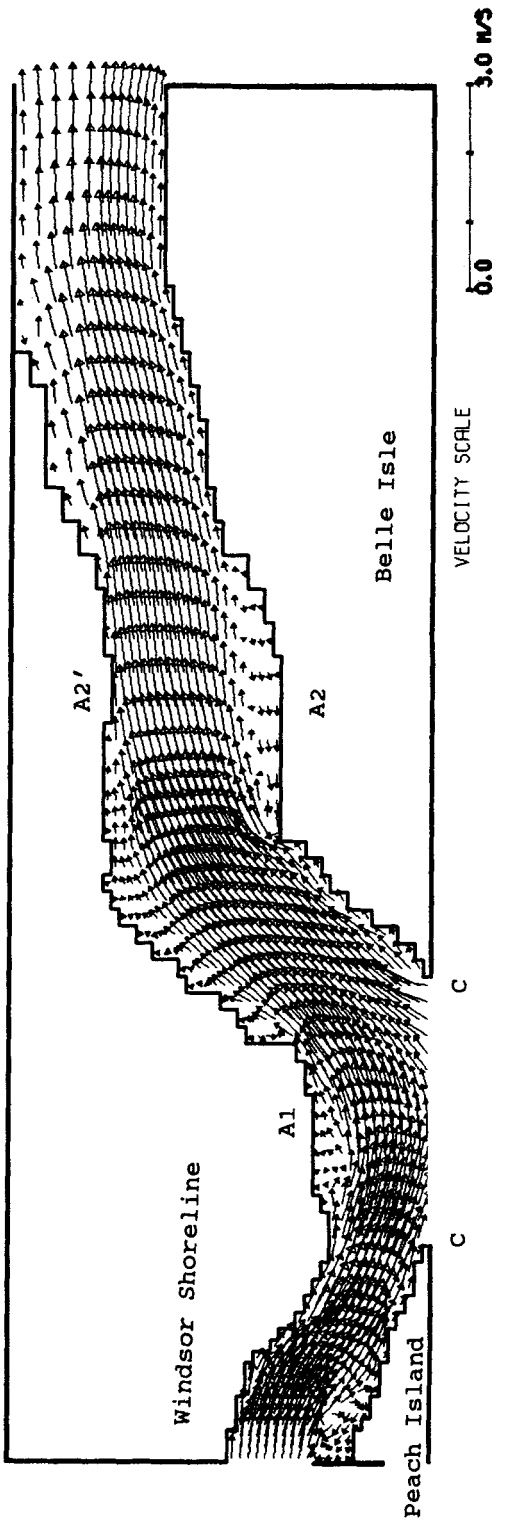

Figure 8. Predicted flow pattern in Fleming Channel by SISUM-9

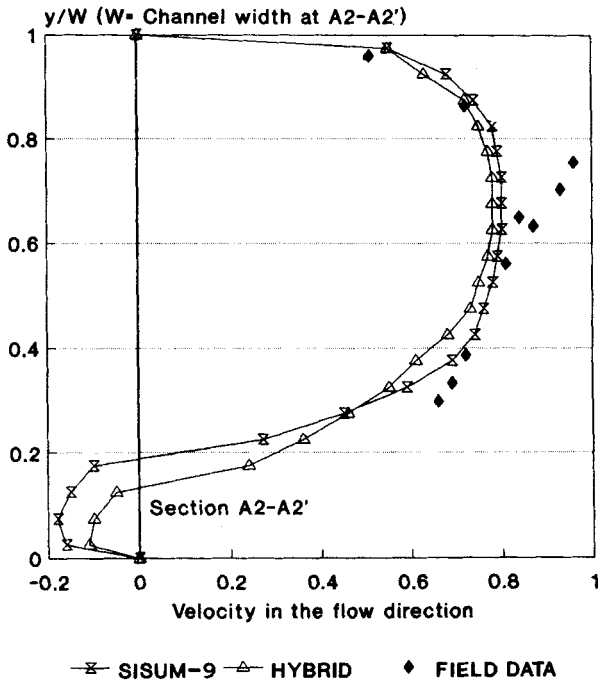

Figure 9. Velocity profiles at section A2–A2'

Figures 10(a)–10(d) present the pollutant contour plots from the hybrid, mixed skew upwind method, SISUM-9 and SISUM-17, respectively, based on the velocity fields predicted by hybrid and SISUM-9. The width of the pollutant belt is assumed to be demarked by the 7% (isoconcentration line (referenced to the inlet concentration). Figure 10(b) shows the results of the mixed skew upwind method (effluent distribution coefficients $=1{\cdot}0$) which is used as the initial field of SISUM-9/17. Comparing this result with the results in Figures 10(c) and 10(d) indicates the ability of the SISUM-9/17 to iteratively decrease the numerical diffusion to the lowest level.

At the upstream end of the reach, the lateral widths of the pollutant belt predicted by the hybrid scheme and SISUM-9/17 are similar, i.e. 40%–50% of the channel width as shown in Figures 10(a), 10(c) and 10(d); however, the deviation between the belt widths rapidly increases as the flow direction deviates from the grid co-ordinate direction. At the down stream end of the reach, both field observations (Figure 7) and SISUM-9/17 gave belt widths in the range of 50%–60% of the channel width, while the hybrid scheme predicted a belt width occupying the whole channel. The major reason for the smearing error is the extreme numerical diffusion in the hybrid method when the streamlines are oblique to the co-ordinate directions in convection-dominated flow. The shape of the pollutant belts simulated by SISUM-9 and SISUM-17 in the whole channel is much closer to the observed turbidity plume (Figure 7) than that predicted by the hybrid scheme.

Comparing the 7% and 52% iso-concentration lines predicted by SISUM-17 (Figure 10(d)) with those given by SISUM-9 (Figure 10(c)) indicates that SISUM-17 produces the sharper concentration gradients and the lower numerical diffusion. However, the deviations between SISUM-9 and SISUM-17 are significantly smaller than those in the case of pure convection due to the refined grid and the realistic gradients.

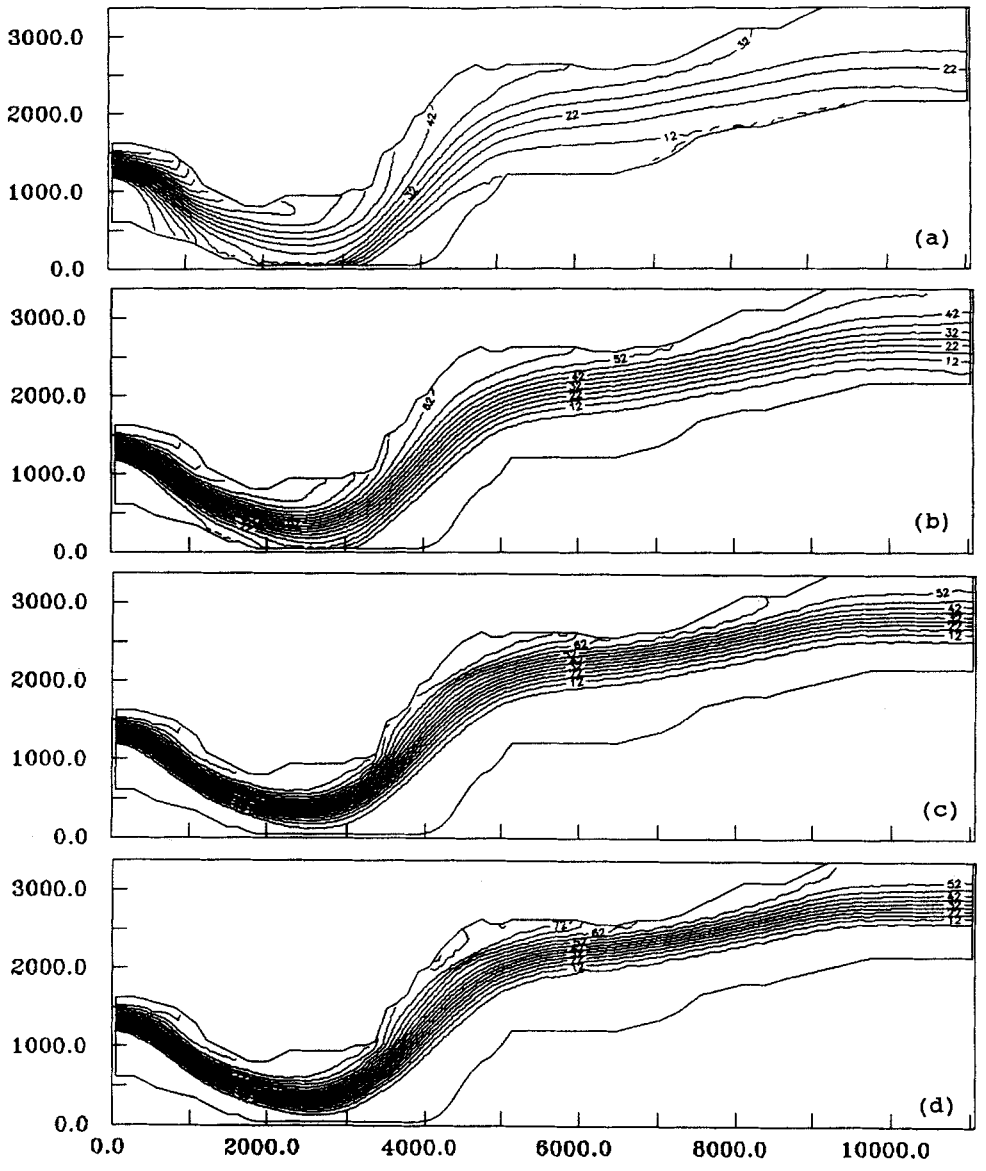

Figure 10. Predicted concentration contour plots by hybrid scheme, mixed skew upwind and SISUM-9/17: (a) prediction by hybrid scheme; (b) prediction by mixed skew upwind; (c) prediction by SISUM-9; and (d) prediction by SISUM-17

Density flows

The final test case is used to check the robustness of SISUM-9 in a problem with a very high stability requirement. The numerical solution of density flow in clarifiers may encounter strong local instabilities;[21] this is due to the extremely low hydraulic loading and very strong density variations which appear in the vertical momentum equation as a large source term.[22] The mathematical model of the clarifier contains a hydrodynamic submodel, a transport submodel, a solids settling velocity equation, an equation of state that relates density and concentration and

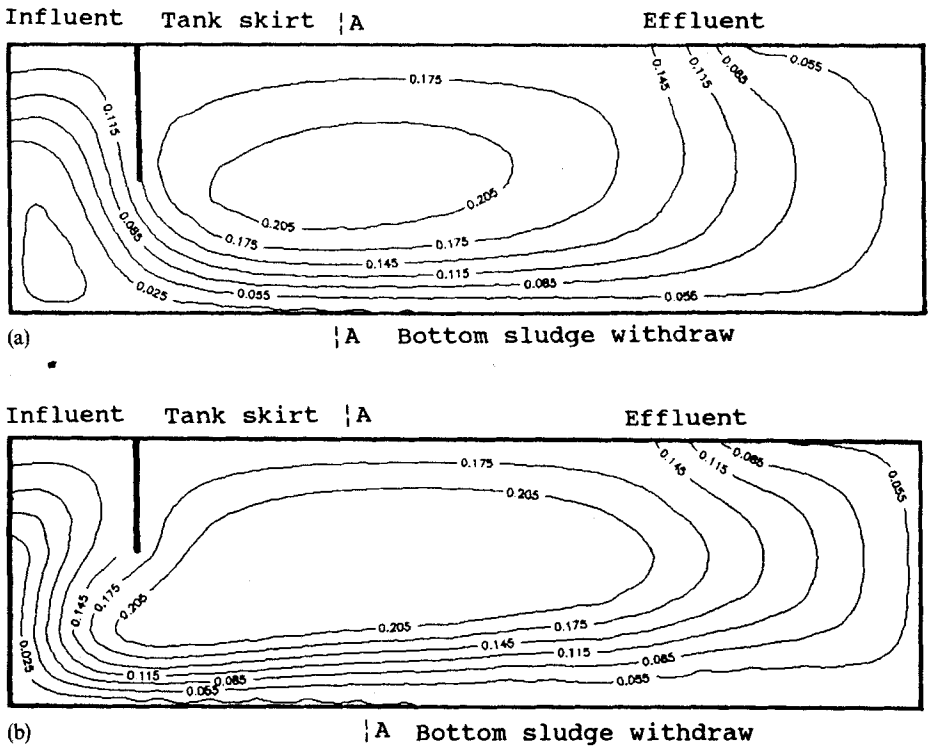

Figure 11. Predicted flow pattern in a circular clarifier by SISUM-9: (a) neutral density; and (b) concentration of inlet solids = 2500 mg l^{-1}

a turbulence k–ε model. The details of the model have been described by DeVantier and Larock[21] and Zhou and McCorquodale.[22]

The simulation considers a prototype circular secondary clarifier with tank radius = 21·0 m, skirt radius = 5·0 m, water depth in the clarifier $H = 5{\cdot}4$ m and height of baffle $H_b = 2{\cdot}75$ m. The total hydraulic loading $Q_0 + Q_r = 3000\ m^3\ h^{-1}$ with a Return Activated Sludge (RAS) ratio = 0·5 (RAS = Q_r/Q_0). Two cases are considered: (a) neutral density; (b) a density flow with inlet solids concentration $C_0 = 2500\ mg\ L^{-1}$. Figures 11(a) and 11(b) show the flow patterns simulated by SISUM-9 for both cases. Figure 12 shows the velocity profiles predicted by SISUM-9 and the hybrid scheme at Section A–A. SISUM-9 is better than the hybrid in reproducing the sharp vertical-velocity gradients for the neutral-density case. The velocity fields of SISUM-9 and the hybrid scheme are almost identical for density flow; this result can be explained by the fact that the density–gravity term in the vertical-momentum equation is an order of magnitude greater than the convection terms.

For the density-flow problem, SISUM-9 required 40 time steps ($\Delta t = 180$ s) each consisting of 40 iterations for the pressure and numerical-diffusion corrections to achieve computational convergence and a steady-state solution. SISUM-9 iterations are carried out simultaneously with the pressure corrections (SIMPLE,[17]). Both SISUM-9 and the hybrid scheme required about the same total number of iterations to reach a steady-state solution for the same convergence criteria ($B_s/Q_0 < 0{\cdot}005$; B_s = summation of the absolute source values for each control volume). The robustness of the method points to the possibility that the skew upwind methods can replace the hybrid scheme in the solution of complex practical engineering problems.

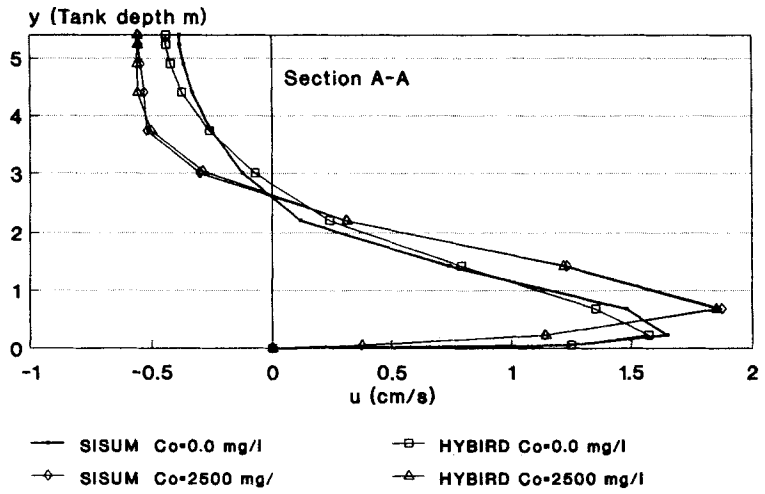

Figure 12. Predicted velocity profiles at section *A–A*

CONCLUSION

The diagonal coefficients in skew upwind schemes are not always dominant and therefore, in the mathematical sense, convergence is not guaranteed; however, physically a realistic solution does exist. The SISUM presents a robust solution procedure for the skew upwind approach. An initial stable solution, based on the mixed skew upwind method with some numerical diffusion, is subsequently relaxed within SISUM until the numerical diffusion is minimized.

The test problems presented here demonstrate that the proposed method has comparable or higher accuracy than the conventional skew upwind schemes with negative coefficients and is reasonably free from numerical instability and over- or under-shooting. The effectiveness of the method was illustrated by the solution of a pollutant transport in the Detroit River. The SISUM, when applied to density flow in clarifiers, was found to be as robust as the hybrid scheme. Comparison of the performance of SISUM with the hybrid scheme in three cases indicates that the SISUM and the conventional SUDS are particularly useful when the convection is primarily responsible for determining the distribution of the variables in curvilinear flow.

ACKNOWLEDGEMENT

This research was supported by a grant from the Natural Sciences and Engineering Research Council of Canada.

APPENDIX I

A test case with over-shooting for SUDS

Figure 13 presents a case with $u_e = u_w = u_n = u_s = 2{\cdot}0$, $v_e = v_w = v_n = v_s = 1{\cdot}0$, $\Delta x = \Delta y = 1{\cdot}0$ and $\alpha = 26{\cdot}6°$ (the angle between velocity vector and horizontal grid). The disadvantage of using the conventional SUDS to estimate convection face values can be shown by a simple numerical testing for this case. For a pure convection problem, equation (9) can be simplified to give

$$2\varphi_e + \varphi_n = 2\varphi_w + \varphi_s. \tag{30}$$

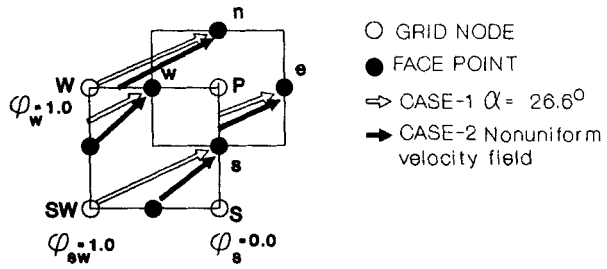

Figure 13. Two interpolation examples for SUDS and SISUM

Conventional SUDS gives the four face values, respectively, as

$$\varphi_w = 0{\cdot}75\varphi_W + 0{\cdot}25\varphi_{SW} \quad \text{(influent w)}, \tag{31}$$

$$\varphi_s = \varphi_{SW} \quad \text{(influent s)}, \tag{32}$$

$$\varphi_n = \varphi_W \quad \text{(effluent n)}, \tag{33}$$

$$\varphi_e = 0{\cdot}75\varphi_P + 0{\cdot}25\varphi_S \quad \text{(effluent e)}. \tag{34}$$

The solution, $\varphi_P = 1{\cdot}333$, shows more than 30% over-shooting in this case. Once the two outlet faces of the control volume are distinguished from the two inlet faces, it is found that one of the outlet surface value expressions, i.e. $\varphi_e = 0{\cdot}75\varphi_P + 0{\cdot}25\varphi_S$, causes the over-shooting in this case. The improved equations (18)–(21) used in SISUM give

$$\varphi_e = 0{\cdot}5\varphi_P + 0{\cdot}5\varphi_s. \tag{35}$$

The solution, $\varphi_P = 1{\cdot}0$, gives no over- or under-shooting. In this case, the value of the effluent φ_e must be 1·0 to maintain mass balance for the same CV regardless for either SISUM or SUDS (see equation (30)). The SISUM gives $\varphi_P = 2{\cdot}0$ $(1{\cdot}0 - 0{\cdot}5\varphi_s)$, which shows that the value of φ_P is related to the influent value of φ_s (face s). However, the SUDS gives $\varphi_P = 1{\cdot}333$ $(1{\cdot}0 - 0{\cdot}25\varphi_S)$, which shows that the value of φ_P is related to the lateral node value φ_S.

A test case with a non-dominate diagonal coefficient

As shown in Figure 13 for a pure convection problem with non-uniform velocity field $u_e = u_w = u_s = 1{\cdot}0$, $u_n = 1{\cdot}5$, $v_w = v_n = v_s = 1{\cdot}0$, $v_e = 0{\cdot}667$ and $\Delta x = \Delta y = 1{\cdot}0$, equation (9) can be simplified to give

$$\varphi_e + \varphi_n = \varphi_w + \varphi_s. \tag{36}$$

Then equations (18)–(21) give four surface values, respectively, as

$$\varphi_w = 0{\cdot}5\varphi_{SW} + 0.5\varphi_W, \tag{37}$$

$$\varphi_s = 0{\cdot}5\varphi_{SW} + 0{\cdot}5\varphi_S, \tag{38}$$

$$\varphi_n = 0{\cdot}75\varphi_W + 0{\cdot}25\varphi_P, \tag{39}$$

$$\varphi_e = 0{\cdot}667\varphi_s + 0{\cdot}333\varphi_P$$
$$= 0{\cdot}3335\varphi_{SW} + 0{\cdot}3335\varphi_S + 0{\cdot}333\varphi_P \tag{40}$$

and the final discretization equation is

$$0{\cdot}583\varphi_P = 0{\cdot}6665\varphi_{SW} + 0{\cdot}1665\varphi_S - 0{\cdot}25\varphi_W . \tag{41}$$

The ratio of the diagonal coefficient to the summation of the absolute value of the off-diagonal coefficients is 0·538 for this case.

REFERENCES

1. S. V. Patankar and D. B. Spalding, 'A calculation procedure for heat, mass and momentum transfer in three-dimensional parabolic flow', *Int. J. Heat Mass Transfer*, **15**, 1787 (1972).
2. G. deVahl Davis and G. D. Mallinson, 'An evaluation of upwind and central difference approximations by a study of recirculation flow', *J. Comp. Fluids*, **4**, 29–43 (1976).
3. G. D. Raithby, 'Skew upstream differencing schemes for problems involving fluid flow', *Comput. methods appl. mech. eng.*, **9**, 153–164, (1976).
4. Y. A. Hassan, J. G. Rice and J. H. Kim, 'A stable mass flow weighted two dimensional skew upwind scheme', *Numer. Heat. Transfer*, **6**, 395–408 (1983).
5. S. Ramadhyani and S. V. Patankar, 'Solution of the convection–diffusion equation by a finite-element method using quadrilateral elements', *J. Numer. Heat Transfer*, **8**, 595–612 (1985).
6. M. J. Raw, 'A new control-volume based finite element procedure for the numerical solution of the fluid flow and scalar transport equations', *Ph.D. Thesis*, University of Waterloo, Waterloo, Ontario, 1985.
7. G. E. Schneider and M. J. Raw, 'A skewed, positive influence coefficient upwinding procedure for control-volume based finite element convection–diffusion computation', *J. Numer. Heat Transfer*, **9**, 1–26 (1985).
8. G. J. Sturgess and S. A. Syed, 'Calculation of confined swirling flows', *AIAA Paper 85-0060*, AIAA 23rd Aerospace Meeting, Reno, Nevada. January, 1985.
9. G. E. Schneider and M. J. Raw, 'Control volume finite-element method for heat transfer and fluid flow using collocated variables – 1. Computational procedure', *J. Numer. Heat Transfer*, **11**, 363–390 (1987).
10. M. Peric, R. Kessler and G. Scheurer, 'Comparison of finite-volume numerical methods with staggered and collocated grids', *Comp. Fluids*, **16**, 389–403 (1988).
11. T. W. H. Sheu, S. M. Lee, K. O. Yang and B. J. Y. Chiou, 'A non-oscillating solution technique for skew upwind and QUICK-family schemes', *Comp. Mech.*, **8**, 365–382 (1991).
12. G. D. Smith, *Numerical Solution of Partial Differential Equations: Finite Difference Methods*, 3rd edn, Clarendon Press, Oxford, 1985.
13. F. Durst and D. Wenneberg, 'Numerical aspects of calculation of confined swirling flows with internal recirculation', *Int. j. numer. methods fluids*, **12**, 203–224 (1991).
14. B. P. Leonard, 'A consistency check for estimating truncation error due to upstream differencing', *Appl. Math. Modelling*, **2**, 239–244 (1978).
15. P. H. Gaskell and A. K. C. Lau, 'Curvature-compensated convective transport: SMART, a new boundedness-preserving transport algorithm', *Int. j. numer. methods fluids*, **8**, 617–641 (1988).
16. B. P. Leonard and S. Mokhtari, 'Beyond first-order upwinding: the ULTRA-SHARP alternative for non-oscillation steady-state simulation of convection', *Int. j. numer. methods eng.*, **30**, 729–766 (1990).
17. S. V. Patankar, *Numerical Heat Transfer and Fluid Flow*, McGraw-Hill, New York, 1980.
18. J. A. McCorquodale and S. Zhou, 'Simulation of pollutant distribution in the St. Lawrence River by application of an advanced numerical model', Report for National Water Research Institute of Canada, University of Windsor, 1992.
19. W. Rodi, *Turbulence Models and their Application in Hydraulics: A State-of-the-Art Review*, International Association for Hydraulic Research, Delft, The Netherlands.
20. U.S. Army Corps of Engineers, *Detroit River Current Studies*, Detroit District Great Lakes and Hydrology Branch, 1974.
21. B. A. DeVantier and B. E. Larock, 'Modeling sediment-induced density current in sedimentation basins', *J. Hydraulic Eng.*, **113**(1), 80–94 (1987).
22. S. Zhou, and J. A. McCorquodale, 'Influence of skirt radius on performance of circular clarifier with density stratification', *Int. j. numer. methods fluids*, **14**, 919–934 (1992).